EUROPEAN ORGANIZATION FOR NUCLEAR RESEARCH

CERN-SPSC
03 April 2009

Status Report
ELECTROMAGNETIC PROCESSES IN STRONG CRYSTALLINE FIELDS

U.I. Uggerhøj[1)]
Department of Physics and Astronomy, Aarhus University, Denmark

NA63

Abstract

Results obtained in the framework of the NA63 experiment [1] at CERN are reported. Analysis of the trident production in the strong crystalline fields of single Ge crystals is completed. Yields in the random ('amorphous') orientation are in good agreement with calculations, and in the aligned case the production is enhanced by about a factor 3 compared to a Ge amorphous material. Results on the formation lengths of several microns for the production of GeV photons from ultrarelativistic electrons have been published. In 2008 we performed a measurement of resonance phenomena in structured targets and studied a possible change in restricted energy loss in thin solid state detectors, for sufficiently high values of the Lorentz factor. The plans for 2009 are to study the 'semi-bare electron' from radiation emission in thin targets and to study the spin-flip mechanisms in radiation emission, relevant for beamstrahlung phenomena in future linear colliders such as CLIC.

[1)] Spokesman, on behalf of the collaboration.

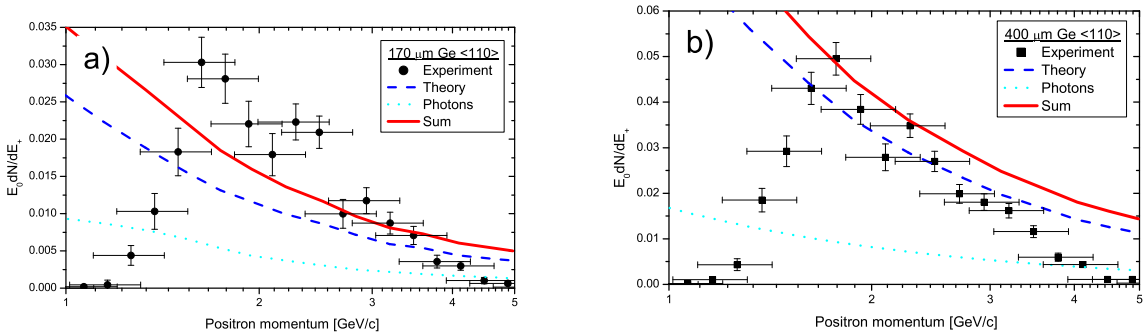

Figure 1: *Differential yield of trident production as a function of the momentum of the produced positron. The points show results obtained for 180 GeV electrons penetrating a) a 170 μm Ge $< 110 >$ crystal oriented in a 'random' direction, and b) a 400 μm Ge $< 110 >$ crystal oriented in a 'random' direction. The experimental data points are shown by filled circles and squares, respectively. The theory of electroproduction $e^- \to e^-e^+e^-$ of Baier and Katkov is shown by the dashed line, and the contribution to triply charged final states from photons produced in the target $e^- \to e^-\gamma \to e^-e^+e^-$ is shown as a dotted line, while the sum of these contributions is shown as the full-drawn line. The vertical error bars are statistical, while the horizontal error bars show the measured, extrapolated momentum resolution.*

1 Results from the run, Oct. 2007

1.1 Trident production in strong crystalline fields

The investigation of trident production in strong crystalline fields by NA63 has led to new calculations of these processes in amorphous [2] and crystalline [3] media, by Baier and Katkov, one of the strongest theoretical groups worldwide within the field of strong field QED. The trident production in strong crystalline fields is a close analogue to the so-called Klein paradox, where an electron impinging on a sufficiently steep potential barrier gives rise to direct pair production, i.e. in total three charged particles are emerging, see e.g. [4, 5, 6]. In this connection, 'sufficiently steep' means of the order the QED critical field, $\mathcal{E}_0 = mc^2/e\lambda_c = 1.32 \cdot 10^{16}$ V/cm, i.e. the rest mass of the electron can be produced by transporting an electron over the distance corresponding to the uncertainty of the location of it, the reduced Compton wavelength of the electron $\lambda_c = \hbar/mc$. Such fields as $\mathcal{E}_0$ are achievable in the rest frame of the penetrating particle, taking advantage of the Lorentz boost and the coherent addition of the screened nuclear fields in crystals, leading to electric fields of magnitude $10^{11} - 10^{12}$ V/cm. More compactly, the relativistic invariance of the parameter

$$\chi = \gamma\mathcal{E}/\mathcal{E}_0 \tag{1}$$

is taken advantage of. See [7, 8, 9] for reviews of similar effects in strong crystalline fields. A review of the experimental setup etc. can be found in the status report of NA63 from 2008 [10]. The analysis has been completed, and the resulting paper is in its final stage of internal review before submission for publication.

In figure 1 is shown the differential yield of trident production as a function of the momentum of the produced positron. The theory of electroproduction (trident) $e^- \to e^-e^+e^-$ in amorphous media of Baier and Katkov [2] is shown for comparison. The same final state of three charged leptons as seen by the detector can appear due to pair production in the solid-state detector (SSD) from a photon generated upstream or in the target itself $e^- \to e^-\gamma \to e^-e^+e^-$. The contribution from this process is shown by the dotted line and the data points must be compared to the sum of these contributions, shown by the full-drawn line. As seen, there is good agreement between theory and experiment, taking into account the uncertainties, in the range of momentum $p_{e^+} \in [1.5; 3.5]$ GeV/c of the produced positrons. Below this range, the geometrical acceptance of the pair spectrometer (a magnetic dipole MDX and two drift chambers, DC5 and DC6) leads to a detection efficiency that drops to zero as the momentum is

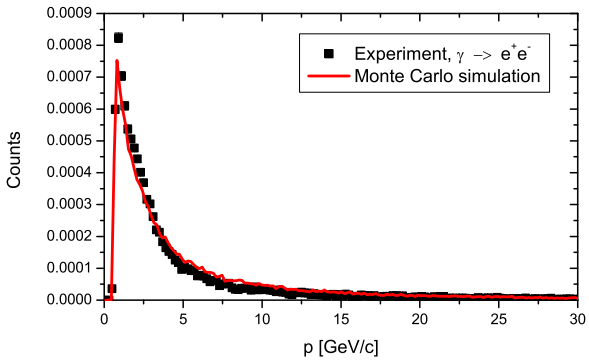

Figure 2: *Yield of pair production as a function of the momentum of the produced positron. The points show results obtained for 100 GeV electrons penetrating a 400 μm thick Ge $<110>$ crystal oriented in the 'random' direction and the line shows simulated values based on the Bethe-Heitler cross sections for radiation emission and pair production, including the limitations in the detection imposed by the geometry of the pair spectrometer.*

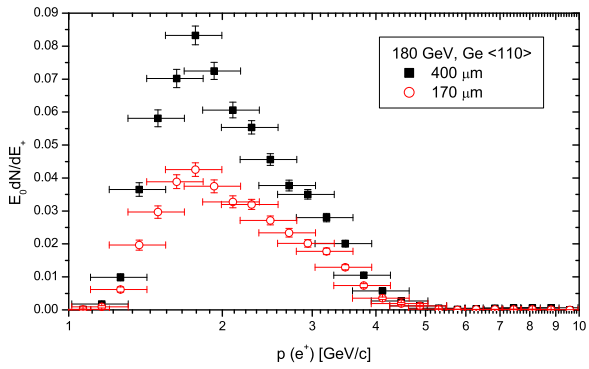

Figure 3: *Differential yield of trident production as a function of the momentum of the produced positron. The points show results obtained for 180 GeV electrons penetrating a 170 μm thick Ge $<110>$ crystal and a 400 μm thick Ge $<110>$ crystal, both oriented in the axial direction.*

reduced. We have also measured the pair production probability for the same orientation of the crystal, verifying the expected values from the Bethe-Heitler cross sections and that the geometrical acceptance is very well reproduced by simulations as seen in figure 2. In the case of tridents, above a momentum of $\simeq 3.5$ GeV, the tracks of the produced particles start to impinge on the same drift chamber cell as the incident electron, leading to reduced efficiency due to the lack of true multi-hit capability of the DCs. We emphasize that these efficiencies are inessential to first order in a comparison of spectra obtained under axially aligned conditions to 'random' alignment, and that the good agreement with expectations obtained for the amorphous case provides a strong basis for the interpretation of the experiment under aligned conditions.

Recent studies have shown that it may be possible to detect the LPM effect in pair production [11], i.e. that the yield of pair production events may be suppressed by multiple scattering of the virtual pair. In NA63 we performed in 2007 a precise measurement of the pair production from 2-100 GeV photons in a Ge crystal, to address this question. Analysis of this data-set - part of which is shown in figure 2 - is on-going.

In figure 3 is shown the yields obtained for the same crystals as in figure 1, but oriented along

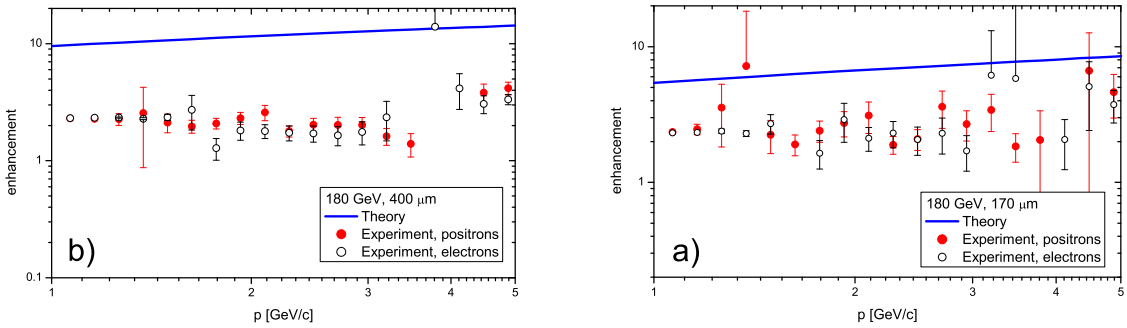

Figure 4: *Differential enhancement of trident production as a function of the momentum of the produced positron (filled circles) and as a function of the momentum of the produced electron (open circles). The points show results obtained for 180 GeV electrons penetrating a) a 170 μm Ge $<110>$ crystal and b) a 400 μm Ge $<110>$ crystal. The lines show the expected enhancement, based on the theory of Baier and Katkov [3].*

the axial direction. As seen, the yield is about a factor 2 larger for the thick crystal, and the spectra obtained are of very similar shape. The correction for the contribution to triply charged final states from photons produced in the target $e^- \rightarrow e^-\gamma \rightarrow e^-e^+e^-$ and converting in the SSD is taken into account by assuming an enhancement for radiation emission that increases linearly from 2.2 to 4.1 in the range of energies 1-20 GeV, as previously measured [12, 13].

In figure 4 is shown the differential enhancement - the ratio of the aligned to the non-aligned trident production probability - versus the momentum of the produced positron for 180 GeV electrons penetrating the 170 μm and 400 μm Ge $<110>$ crystals. The enhancement is about a factor 3 for all momenta investigated, which is below theoretical results [3] of $\eta \approx 6-8$ for the same configuration, results that on the other hand do not include 'diluting' effects such as angular spread. Moreover, as the enhancement does not depend significantly on the thickness of the crystal, the dominant process in the strong field case could be interpreted to be through a virtual intermediate photon, since the dependence on the square of the thickness for the sequential process would yield a significant difference in enhancement, if that process dominated. This is in contrast to theory, that predicts a relatively small contribution from the direct channel - about 20% at the lowest positron energy - in the case of the aligned crystal [3]. However, an alternative interpretation of the experiment could be that the 400 μm Ge $<110>$ crystal was not perfectly aligned and therefore gave a smaller enhancement than when properly aligned. We estimate the accuracy of the alignment procedure to be about 25 μrad, significantly smaller than the relevant angle for strong field effects, $\vartheta_0 \simeq 0.5$ mrad. This alternative therefore seems unlikely. On the other hand, the dechanneling length for electrons amounts to approximately 100 μm at 1 GeV which means that coherence may be lost for crystal thicknesses much larger than that. Therefore, the enhancement measured for the thicker crystal is not as reliable as for the thin one.

Also shown in figure 4 with open circles is the differential enhancement as a function of the momentum of the produced electrons for 180 GeV electrons penetrating a 170 μm Ge $<110>$ crystal. The nice, almost exact agreement between the two modes of detection and analysis, focusing on the produced electron or positron, respectively, shows that systematic uncertainties affecting the results are likely to be small. Furthermore, it shows that effects such as energy loss of the produced particles in the remaining part of the crystal downstream the production point, is likely to be small as electrons tend to suffer much more energy loss close to the axis than positrons. A similar conclusion is reached for the 400 μm thick crystal.

2 Results from the run, Oct. 2008

The NA63 experiment was initially given 11 days of beamtime in the H4 zone of the CERN SPS in October 2008. However, due to the unfortunate incident in the CERN LHC, this beamtime was severely reduced to 40% to allocate resources to a quick recovery of the LHC. Moreover, a ground error in the B3 magnet arose on the first day, leading to another 12 hours lost, a reduction to about a quarter of the intensity and a limitation on the maximum energy achievable of 200 GeV. In this connection, we are grateful to the SPS beam physicists, Ilias Efthymiopoulos and Bruno Chauchaix, for finding on a short notice an optics solution that could give us at least some beam. With these restrictions, NA63 investigated 2 phenomena:

1. Change in restricted energy loss in thin solid state detectors
2. Formation length effects in structured (sandwich) targets

albeit at a much reduced level of accuracy compared to planning.

2.1 Change in restricted energy loss in thin solid state detectors

In a measurement performed 30 years ago, Ogle and collaborators [14] investigated a reduction in energy deposition in a thin solid state detector, 100 μm of Si. They reported a reduction in restricted energy loss for values of the Lorentz factor exceeding

$$\gamma_c = \frac{a\omega_p}{2c} \tag{2}$$

based on four data points in the region $\gamma \in [1.6 \cdot 10^4; 1.0 \cdot 10^5]$, where $\gamma_c = 7.9 \cdot 10^3$. In equation (2) a is the thickness of the detector and ω_p the plasma frequency. Their theoretical approach was based on an argument with minimum longitudinal momentum transfer, similar to studies of the formation zone. Although their theory is questionable, it seems to be supported by their measured values.

On the other hand, one can use a characteristic length for the generation of transition radiation as e.g. defined in [15] or [16]

$$l_c = \frac{2\gamma^2 c}{\omega} = \frac{2\gamma c}{\omega_p} \tag{3}$$

with $\omega = \gamma\omega_p$. From equation (3) appears that the full screening of the field of the penetrating particle takes place only after a distance l_c, i.e. for distances shorter than this the density effect may not be fully active for the restricted energy loss. This would result in an *increased* energy deposition for values of the Lorentz factor exceeding exactly the same as given in equation (2).

In the October 2008 run, we studied this possible change of energy deposition in thin solid state detectors. Using electron beams of energy 40-180 GeV passing a target of 7% X_0 and being deflected in an MBPL magnet, we generated electrons of energies in the interval between about 10 GeV and 174 GeV, tagged by means of the signal in the lead glass detector. By moving the thin solid state detector stepwise across the deflected electron beam as indicated in figure 5, we obtained a spectrum of 12 energy points (compared to the planned 50 points in the range of energies 0.5-250 GeV) in the few days of beam time. Moreover, the measurement accuracy was not optimized due to lack of time.

The effective thickness of the detector has been determined by a comparison of theory of Sternheimer and Peierls [17] to data obtained at ASTRID (Aarhus STorage RIng Denmark). Calibration of the detector was for both measurements done by use of x-rays from ^{133}Ba and the possible overall deviation of the CERN data with respect to the ASTRID data resulting from the calibrations is less than 1 keV. The theoretical lines shown in figure 6 are based on Sternheimer and Peierl's theory [17] (full line), the modified energy loss suggested by Ogle and collaborators [14] in their equation (2) (dashed line) and the modified energy loss suggested by Ogle and collaborators [14] from physical arguments based on loss of coherence (dot-dashed line). The latter has been produced by using their experimentally verified curve obtained for a 101 μm thin SSD and scaling the thickness dependence based on the notion of a critical value of the Lorentz factor, $\gamma_c = a\omega_0/2c$, above which the effect appears. The MPEL has generally been measured to an accuracy of a few percent and it is clear from figure 6 that the agreement with the modified physical model suggested by Ogle and collaborators [14] (dot-dashed line) is poor. On the other hand, an increase of a few percent for Lorentz factors above γ_c cannot be excluded, nor can the

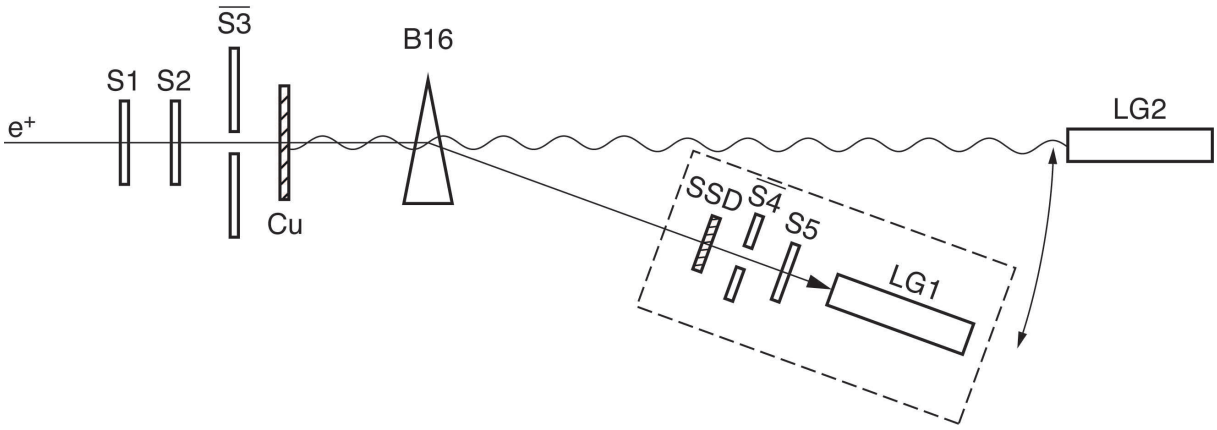

Figure 5: *A schematical drawing of the setup used in the experiment at CERN. The total length of the setup is about 20 m.*

alternative model suggested by Ogle and collaborators [14] (dashed line) which for Lorentz factors in the vicinity of γ_c has the same tendency as loss of the density effect.

2.2 Formation length effects in structured (sandwich) targets

By assembling a target of tantalum sub-targets, interspersed with spacers for which the radiation length is significantly smaller, so-called structured target phenomena can be investigated. These phenomena arise due to the large longitudinal extent of the formation zone,

$$l_{\mathrm{f}} = \frac{2\gamma^2 c}{\omega} \tag{4}$$

an extent that for sufficiently high electron energies and sufficiently small photon energies, may exceed the dimension of the tantalum sub-targets, or span across the spacers. This leads to suppression or enhancement, depending on photon energies.

Two target configurations were used (identified below by the label given in parenthesis): (Ta10Air90) A structured target of 10 layers of 10 μm thickness tantalum with 90 μm air gaps and a reference target (Ta100) consisting of a single foil of 100 μm Ta. The air gaps were kept equidistant by the use of 90 ± 3 μm thick spacers with Ø 15 mm holes made from phosphor-bronze, a mechanically stable material that is machinable. The targets of 50×50 mm^2 were mounted in a holder with an open area of 15 mm in diameter and the outermost holders were made from 5 mm thick stainless steel, also with Ø 15 mm holes, to provide pressure to the stack of foils situated between them. By the choice of number of sub-targets, the structured target has the same thickness in units of radiation lengths as the reference target Ta100, i.e. ratios of radiation probabilities are expected not to be influenced by multi-photon emission effects. The background measured with an empty target with identical target holders with Ø 15 mm holes has been subtracted from the data. The background corresponds to about 2% of a radiation length.

Operating a BGO detector (described in [10]) in the high energy photon beam, required special care. Using the recommended value of high-voltage (HV) from the supplier of the XP 3330 photomultiplier (PM) in the range 700-1100 Volts, lead to complete saturation for photon energies above a few GeV. This resulted in a strong peak of radiation in the region of calibrated photon energies of 0.5 GeV, most likely because the light-yield was so high that the PM could not sustain the voltage during the time of integration of the pulse. Instead, the HV was reduced to 400 Volts where no such artefacts appeared. Moreover, preceding and subsequent testing with 100-580 MeV electrons from the ASTRID storage ring in Aarhus, showed that even with this low HV, the signal from the BGO detector was linear to better than 1% with energy. The relative RMS width of the BGO signal was about 5%.

In figure 7 we show the enhancement of radiation emission for the structured target, Ta10Air90, compared to the homogeneous target, Ta100. Using the ratio eliminates effects originating from inefficiency or theoretical normalization problems, at least to first order. The enhancement is clearly visible,

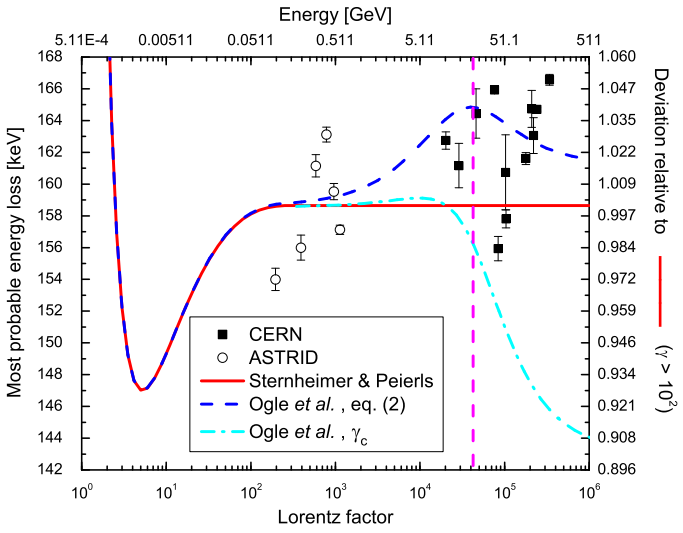

Figure 6: *Measured values for the Most Probable Energy Loss (MPEL) in a 545 μm thick silicon detector, with statistical uncertainties. The full line shows the theoretical curve based on Sternheimer and Peierl's theory [17], the dashed curve the modified energy loss suggested by Ogle and collaborators [14] in their equation (2) and the dot-dashed curve the modified energy loss suggested by Ogle and collaborators [14] from physical arguments based on loss of coherence. The vertical dashed line shows γ_c.*

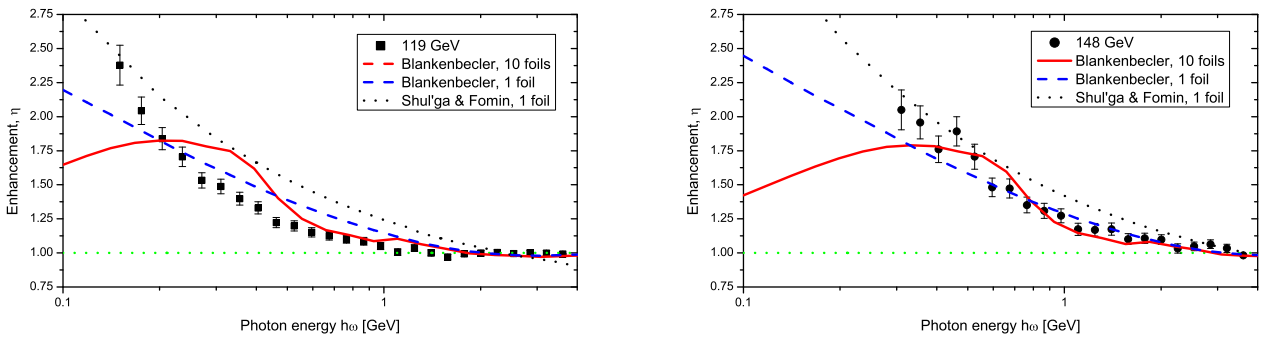

Figure 7: Enhancement of radiation emission for the structured target, Ta10Air90, compared to the homogeneous target, Ta100. The filled squares show experimental results for 119 GeV. The solid and dashed lines show the enhancement calculated using the theory of Blankenbecler [18, 19], with the solid line for 10 target segments each separated by 90 μm from the adjacent foils and the dashed line for each segment acting alone. The dotted line shows the enhancement calculated using the theory of Shul'ga and Fomin [**?**].

and in fair agreement with expectations. The enhancement for 148 GeV should appear at a photon energy higher than for 119 GeV as is also observed. Except for a few low-energy data points, there is good overall agreement between experiment and the theory of Blankenbecler [18, 19], in particular for 148 GeV. However, the difference between the structured target effect as shown by the solid line and the effect of the formation length exceeding the target thickness shown with dashed and dotted lines, is too small to be clearly demonstrated experimentally for photon energies in the range detected. We therefore cannot claim to have measured a structured target effect, but in either case the enhancement is based on the existence of a formation length.

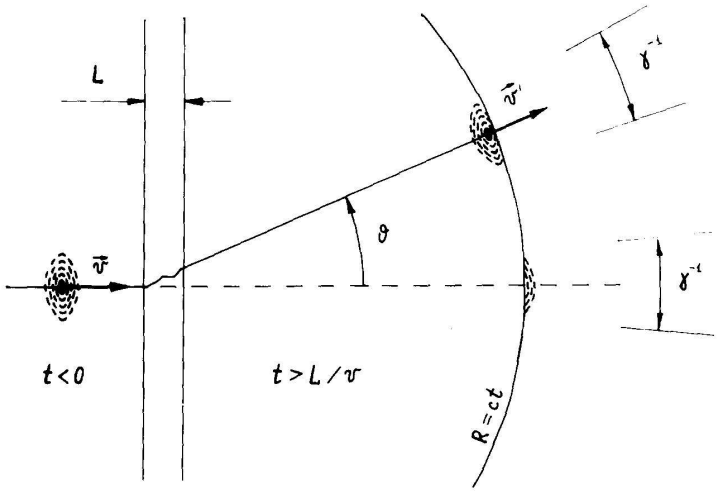

Figure 8: *A sketch of an electron with a Lorentz contracted Coulomb field entering from the left, and impinging on a target of thickness L. As a result of interaction(s) in the target, the direction of the particle changes by an angle ϑ. Due to the difference between the velocity of the particle v and the velocity with which information about the changed direction of the penetrating particle spreads out, the velocity of light c, the scattered electron does not completely restore its field components until after a length of travel of approximately $2\gamma^2 c/\omega$. It is therefore within this zone in a 'semi-bare' state, and may radiate at a reduced level upon subsequent collisions. Adapted from [20].*

3 Plans for the runs, 2009

NA63 has been allocated beam time in June and October of 2009, and

1. The 'semi-bare' electron
2. Spin-flip radiation emission

3.1 Plans for the run, June 2009

3.1.1 The 'semi-bare' electron

After scattering, the relativistic electron stays for a long time in a 'semi-bare' state, partly without its normal Coulomb field, and consequently, during subsequent collisions of this electron with the constituents of the medium the radiation emission is suppressed compared to the case when the field of the electron is at equilibrium. Although this interpretation is open to questions [21], the resulting observable phenomenon is not: The radiation emission is predicted to be proportional to the logarithm of the thickness, for sufficiently high electron energies and suitable photon energies $\hbar\omega$ (where suitable photon energies means higher than the threshold for the appearance of the longitudinal density effect, $\gamma\hbar\omega_p < \hbar\omega$, and lower than the photon energy where the corresponding formation length equals the target thickness $\hbar\omega < 2\gamma^2\hbar c/\Delta t$). At the same time, the target thicknesses must be in the range of a few percent of a radiation length, but above $\alpha X_0/4\pi$ corresponding to 2.4 microns of Ta below which the target acts as a single scatterer and gives a Bethe-Heitler spectrum. A calculation for 207 GeV electrons impinging on Tantalum targets with thicknesses from 5 to 200 microns is shown in figure 9.

We have prepared a sequence of targets, mounted on a remote-controlled rotation stage, with Ta target segments as those shown in figure 9, assembled with 1 mm distance (to avoid 'structured target resonances') and total thicknesses as close as possible to 2.5%X_0 to eliminate the influence of pile-up. Furthermore, 80 pieces of 25 micron thick aluminium (where $\alpha X_0/4\pi \simeq 52$ μm) sheets assembled in a similar configuration should provide a useful 'reference', yielding a Bethe-Heitler spectrum. Finally, given sufficiently high electron energies and a lower threshold for photon detection of $\lesssim 100$ MeV, the possibility of observing the 'structured target resonances' is open, with suitably arranged targets.

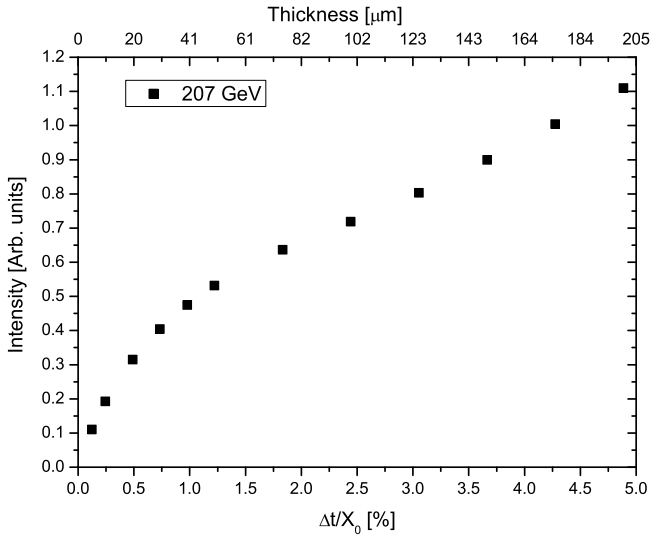

Figure 9: *The radiation intensity of 150-220 MeV photons emitted by 207 GeV electrons passing targets of thicknesses from 5 to 200 microns. For small thicknesses, the radiation emission depends logarithmically on the thickness.*

3.2 Plans for the run, Oct. 2009

3.2.1 Spin-flip radiation emission

As shown in [9], the results obtained in previous experiments within the NA43 collaboration on the influence of spin on the emission spectrum [22], see also [23, 24], are relevant for the understanding of the mechanisms of beamstrahlung in future linear colliders such as CLIC. In the case of collisions of polarized beams, the depolarization during the collision is important to understand correctly, in order to be able to accurately extract what the polarization was at the moment of collision, from polarimeters positioned up- and downstream the collision point [25]. The models presently in use for these predictions, are based on the same strong field QED methods as those that are tested using crystals. As originally suggested in our proposal [1], we aim to measure the contribution from spin to the radiation emission in the case of electrons and positrons penetrating single crystals along axial and planar directions, thus enhancing our understanding of these processes that were so far limited to electrons in the axial direction of tungsten crystals, without the possibility of deconvoluting the single-photon content by use of a pair spectrometer.

The effect of spin on the radiation for near-critical magnitudes of the field in the rest-frame of the emitting electron has been tested only in the axial case and for a relatively thick crystal. This may be extended to investigate planar as well as axial effects for thin crystals and for both electrons and positrons. The planar case for positrons is much more well-defined since the number of initially channeled particles is high, about 90% as opposed to barely 5% for axially channeled electrons.

Asymptotically, the spin contribution becomes $\xi dN/d\xi \propto (\xi^7/(1-\xi))^{1/3} \cdot \chi^{2/3}$ for $\chi \to \infty$ such that it is strongly peaked at the upper end of the spectrum. An example is given in fig. 10 where the value of χ is set to 100.

The study of radiation emission for high values of χ is relevant for e.g. beamstrahlung. The emission of beamstrahlung can be expressed as a function of χ which for the Stanford Linear Collider (SLC) is small $\simeq 10^{-3}$ but of the order unity for the next generation linear colliders [26, 27]. The influence of spin on the radiation process [22, 28] becomes the dominant factor once or χ becomes much higher than 1. We wish to do a measurement in two 'cleaner' cases, namely where the crystal is thin enough to make pile-up insignificant and in the case of planar channeled positrons, where the transverse potential is well approximated by a harmonic potential.

For a future linear collider operating in the 'quantum regime', the beamstrahlung spectrum be-

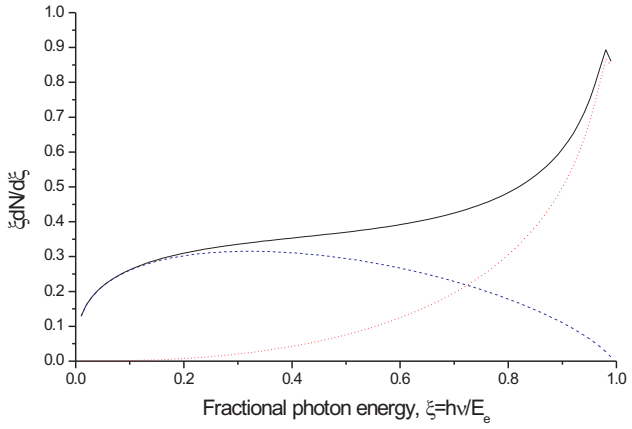

Figure 10: *Synchrotron radiation in a strong field, where the full line is the total spectrum, the dash-dotted line shows the contribution from the spin and the dashed line is obtained by neglecting the spin as in [8]. The value of χ is set to 100.*

comes similar to the spectrum shown in fig. 10, see the full-drawn line in fig. 11.

3.3 Experimental details

This experiment requires aligned thin crystals of heavy elements like tungsten or iridium as well as the operation of 6 drift chambers for angular and position selections on the crystals, photon tagging as well as to produce ‘single-photon spectra by means of reconstruction of the photon momentum in a magnetic pair spectrometer. This spectrometer - which is based on conversion of the photons into electron-positron pairs and subsequent magnetic momentum analysis - has been operated before by NA63 as e.g. shown in figure 2.

3.4 Beam time

As the crystals must be aligned to an axial orientation, the alignment procedure - even with a pre-aligned crystal - is expected to take about half a day for each crystal. In particular, we aim to include the pair spectrometer based on the MDX and two driftchambers, that was also used for the trident experiment in 2007, combined with a thin (about 0.1 X_0) conversion target of amorphous copper, thus enabling us to ’deconvolute’ the single-photon content of the photons emitted from the aligned crystals by measuring the energy of the converted photons. As primary targets, we will use germanium, iridium and tungsten crystals. The most important region of emission is the high energy photons, i.e. $\xi \gtrsim 0.6$. In 0.1 mm W, oriented in the ‘random’ direction where it behaves as an amorphous foil of thickness $\simeq 3\%X_0$, the fraction of photons emitted above $\xi = 0.6$ is 1.4% of the number of incident electrons. The typical background radiation from drift chamber windows, scintillators and air-gaps corresponds to slightly less than $1\%X_0$, estimated from previous runs in H4. Aiming for a total of 5e4 events with $\xi > 0.6$, a run in the ‘random’ orientation requires 7e6 electrons. With a total reconstruction efficiency of tracks through the magnetic pair spectrometer of about 50% in this energy region (highly asymmetric pairs where e.g. the positron takes more than 90% of the energy cannot be detected), and a conversion efficiency of the photons to detectable pairs of 10% (must be kept relatively low to avoid radiation generated by the pair) 70e6 electrons are needed. Using a pessimistic down-time of 50% of the accelerator-chain and counting 4 bursts a minute with 50k electrons, this target takes about 12 hours to complete satisfactory statistics. A run with an oriented target, however, takes considerably longer, since the statistics must allow for off-line angular selections in position and angle. Three oriented crystals of germanium, iridium and tungsten, in random, planar and axial orientations is thus estimated to require run for a total of 15 days, leaving 5 days for the installation and calibration.

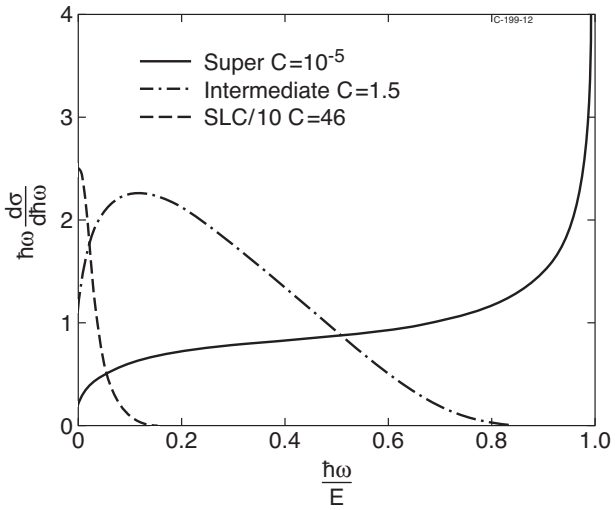

Figure 11: *Three examples of beamstrahlung power spectra where the horizontal scale is the fractional photon energy and the constant* C *here is approximately equal to* $1/\chi$*. Adapted from [29].*

4 Status of publications

The CERN NA63 collaboration has so far resulted in the following publications:

1. T. Virkus, U.I. Uggerhøj, H. Knudsen, S. Ballestrero, A. Mangiarotti, P. Sona, T.J. Ketel, A. Dizdar, S. Kartal and C. Pagliarone (CERN NA63): *Direct measurement of the Chudakov effect*, Phys. Rev. Lett. **100**, 164802 (2008)
2. H.D. Thomsen, K. Kirsebom, H. Knudsen, E. Uggerhøj, U.I. Uggerhøj, P. Sona, A. Mangiarotti, T.J. Ketel, A. Dizdar, M. Dalton, S. Ballestrero and S. Connell (CERN NA63): *On the macroscopic formation length for GeV photons*, Phys. Lett. B **672**, 323 (2009)
3. J. Esberg, K. Kirsebom, H. Knudsen, H.D. Thomsen, E. Uggerhøj, U.I. Uggerhøj, P. Sona, A. Mangiarotti,, T.J. Ketel, A. Dizdar, M. Dalton, S. Ballestrero, S. Connell (CERN NA63): *Experimental investigation of a Klein paradox analogue for elementary particles - strong field trident production*, in preparation for submission April 2009
4. K.R. Hansen, J. Esberg, H. Knudsen, M. Lund, H.D. Thomsen, U.I. Uggerhøj, S.P. Møller, P. Sona, A. Mangiarotti, T.J. Ketel, A. Dizdar and S. Ballestrero (CERN NA63): *Restricted energy loss of ultrarelativistic particles in thin targets - a search for deviations from constancy*, in preparation for submission May 2009

References

[1] J.U. Andersen *et al.* (CERN NA63), CERN-SPSC-2005-030, SPSC-P-327 and CERN-SPSC-2005-016, SPSC-I-232

[2] V.N. Baier and V.M. Katkov, "Electroproduction of electron-positron pair in a medium", JETP Lett. **88**, 80-84 (2008), arXiv:0805.0456

[3] V.N. Baier and V.M. Katkov, "Electroproduction of electron-positron pair in oriented crystal at high energy", subm. Phys. Lett. B (2009), arXiv:0810.1802

[4] W. Greiner, B. Müller and J. Rafelski - *Quantum Electrodynamics of Strong Fields*, Springer, Berlin 1985

[5] H. Nitta, T. Kudo and H. Minowa, Am. J. Phys. **67**, 966 (1999)

[6] P. Krekora, Q. Su and R. Grobe, Phys. Rev. Lett. **92**, 040406 (2004)

[7] V.N. Baier, V.M. Katkov and V.M. Strakhovenko, *Electromagnetic Processes at High Energies in Oriented Single Crystals*, World Scientific 1998.

[8] A.H. Sørensen, Proc. NATO ASI **255**, 91, Plenum, 1991, reprinted in Nucl. Instr. Meth. B **119**, 1 (1996)

[9] U.I. Uggerhøj, Rev. Mod. Phys. **77**, 1131 (2005)

[10] U.I. Uggerhøj (NA63), Electromagnetic processes in strong crystalline fields, CERN-SPSC-2008-012; SPSC-SR-030, Status Report 2008

[11] V. N. Baier, V. M. Katkov, *Opportunity to study the LPM effect in oriented crystal at GeV energy*, arXiv:07113670

[12] A. Belkacem *et al.*, Phys. Lett. B **177**, 211 (1986)

[13] R. Medenwaldt *et al.*, Phys. Lett. B **242**, 517-522 (1990)

[14] W. Ogle, P. Goldstone, C. Gruhn and C. Maggiore, Phys. Rev. Lett. **40**, 1242 (1978)

[15] J.D. Jackson - *Classical Electrodynamics*, Wiley, 1975

[16] A.I. Akhiezer and N.F. Shul'ga - *High Energy Electrodynamics in Matter*, Gordon and Breach, 1996

[17] R. M. Sternheimer and R. F. Peierls, Phys. Rev. B **3**, 3681 (1971)

[18] R. Blankenbecler, Phys. Rev. D **55**, 190 (1997)

[19] R. Blankenbecler, Phys. Rev. D **55**, 2441 (1997)

[20] S.P. Fomin and N.F. Shul'ga, Phys. Lett. A **114**, 148 (1986)

[21] B.M. Bolotovskii and A.V. Serov, Phys. Usp. **40**, 1055 (1997)

[22] K. Kirsebom, U. Mikkelsen, E. Uggerhj, K. Elsener, S. Ballestrero, P. Sona and Z.Z. Vilakazi, Phys. Rev. Lett. **87**, 054801 (2001)

[23] A.V. Korol, A.V. Solov'yov and W. Greiner, Journ. Phys. G **28**, 627 (2002)

[24] V. N. Baier, V. M. Katkov, Nucl. Instr. Meth. B **266**, 3828 (2008)

[25] I. Bailey, presentation at 'Advanced QED methods for future accelerators', Cockcroft Institute 3rd-4th March 2009, http://qed.dl.ac.uk/programme.html

[26] A.V. Solov'yov, A. Schäfer and C. Hofmann, Phys. Rev. E **47**, 2860 (1993)

[27] A.V. Solov'yov and A. Schäfer, Phys. Rev. E **48**, 1404 (1993)

[28] A. Kh. Khokonov *et al.*, Technical Physics **47**, 1413 (2002); A. Korol, A.V. Solov'yov and W. Greiner, J. Phys.G: Nucl. Part. Phys. **28** , 627 (2002)

[29] R. Blankenbecler and S.D. Drell, Phys. Rev. D **36**, 277 (1987)